



HAL
open science

**In utero onset of long QT syndrome with
atrioventricular block and spontaneous or
lidocaine-induced ventricular tachycardia: Compound
effects of hERG pore region mutation and SCN5A
N-terminus variant**

Ming-Tai Lin, Mei-Hwan Wu, Chien-Chih Chang, Shuenn-Nan Chiu, Olivier Thériault, Hai Huang, Georges Christé, Eckhard Ficker, Mohamed Chahine

► **To cite this version:**

Ming-Tai Lin, Mei-Hwan Wu, Chien-Chih Chang, Shuenn-Nan Chiu, Olivier Thériault, et al.. In utero onset of long QT syndrome with atrioventricular block and spontaneous or lidocaine-induced ventricular tachycardia: Compound effects of hERG pore region mutation and SCN5A N-terminus variant: hERG Mutation and SCN5A Variant in LQTS. *Heart Rhythm*, 2009, 5 (11), pp.1567-1574. 10.1016/j.hrthm.2008.08.010 . inserm-00381036

HAL Id: inserm-00381036

<https://inserm.hal.science/inserm-00381036>

Submitted on 5 May 2009

HAL is a multi-disciplinary open access archive for the deposit and dissemination of scientific research documents, whether they are published or not. The documents may come from teaching and research institutions in France or abroad, or from public or private research centers.

L'archive ouverte pluridisciplinaire **HAL**, est destinée au dépôt et à la diffusion de documents scientifiques de niveau recherche, publiés ou non, émanant des établissements d'enseignement et de recherche français ou étrangers, des laboratoires publics ou privés.

In Utero Onset of Long QT Syndrome with Atrioventricular Block and Spontaneous or Lidocaine-induced Ventricular Tachycardia: compound effects of hERG pore-region mutation and SCN5A N-terminus variant

Ming-Tai Lin^a, Mei-Hwan Wu^a, Chien-Chih Chang^{a,b}, Shuenn-Nan Chiu^a, Olivier Thériault^c, Hai Huang^c Georges Christé^d, Eckhard Ficker^e and Mohamed Chahine^{c,f}

Department of Pediatrics^a, National Taiwan University Hospital and College of Medicine, National Taiwan University, Taipei, Taiwan

Department of Pediatrics, Ming-Shen General Hospital^b, Taoyuan, Taiwan

Le Centre de recherche Université Laval Robert-Giffard^c, Québec, (Québec) G1J 2G3
INSERM^d, Lyon, France, Case Western Reservation University^e, Cleveland, USA and
Department of Medicine, Laval University^f, Quebec, (Quebec) Canada, G1K 7P4

Correspondence: Mei-Hwan Wu, MD, Department of Pediatrics, National Taiwan University Hospital, No. 7, Chung-Shen South Road, Taipei, Taiwan 100

Fax: 886-2-23412601

Email: wumh@ntu.edu.tw

Running title: hERG mutation and SCN5A variant in LQTS

ABSTRACT

BACKGROUND Mexiletine may protect patients with long QT syndrome (LQTS) type 3 from arrhythmias. However, we had found an unusual in utero presentation of intermittent atrioventricular block and ventricular tachycardia, spontaneous or lidocaine-induced, in a fetus and his sibling with LQTS.

OBJECTIVE This study was to investigate the underlying channelopathy and functional alteration.

METHODS Mutations were searched in KCNQ1, HERG, KCNE1, KCNE2, and SCN5A genes. In expressed mutants, whole-cell voltage clamp defined the electrophysiological properties.

RESULTS Novel missense mutations involving hERG (F627L) at the pore region and SCN5A (R43Q) at the N-terminus were found in the proband and family members with prolonged QT interval. In oocytes injected with mRNA encoding hERG/ F627L, almost zero K⁺ currents were elicited and in co-injected oocytes, the currents were decreased to half. In tsA201 cells transfected with SCN5A/R43Q, though the baseline kinetics of the Na current was similar to wild type, lidocaine caused a unique hyperpolarizing shift of the activation and increased the availability of Na currents at resting voltages. The window currents were also enhanced due to a right shift of steady-state inactivation. These electrophysiological alterations after lidocaine may lead to the development of ventricular tachycardia.

CONCLUSIONS We have identified a novel hERG/F627L mutation that results in LQTS with fetal onset of atrioventricular block and ventricular tachycardia. Besides, a coexisting SCN5A/R43Q variant, although it *per se* does not prolong repolarization,

attributes the development of ventricular tachyarrhythmias after lidocaine. Patients with such latent lidocaine-induced phenotype given lidocaine or mexiletine may be at risk.

KEYWORDS Congenital long QT syndrome; Atrioventricular block; Ventricular tachycardia; SCN5A; hERG; Mutation; Variant; Lidocaine

Abbreviation:

AV : atrioventricular

LQTS: long QT syndrome

PCR: polymerase chain reaction

SSCP: Single-strand conformational polymorphism

INTRODUCTION

Congenital long QT syndrome (LQTS) is an inherited cardiac channelopathy. Patients are at high risk of potentially fatal ventricular tachyarrhythmias, especially torsades de pointes, due to abnormally prolonged repolarization.^{1,2} Patients with ventricular tachyarrhythmias during the fetal or perinatal stages may be associated with functional atrioventricular (AV) block and carry a worse prognosis.^{3,4} Mutations have been identified in 10 genes encoding cardiac ion channels and their auxiliary subunits, which are involved in shaping the cardiac action potential [i.e., KCNQ1 (LQTS1), hERG (LQTS2), SCN5A (LQTS3), ANK2 (LQTS4), KCNE1 (LQTS5), KCNE2 (LQTS6), KCNJ2 (LQTS7), CACNA1C (LQTS8), CAV3 (LQTS9), SCN4B (LQTS10)]. The majority of mutations are in the KCNQ1 (30-35%), hERG (25-30%) and SCN5A (5-10%) genes.¹⁻⁵ The KCNQ1/KCNE1 and hERG code for the voltage-gated potassium channels (I_{Ks} and I_{Kr} , respectively), and SCN5A encodes a sodium channel α -subunit.^{6,7} Further diversity appears when an increasing number of compound heterozygote mutations within one or even two different LQTS genes have been reported.⁹⁻¹² Such compound mutations may increase the risk of arrhythmia and are associated with more severe forms of LQTS. But, to date, only limited studies have reported the functional alterations.

Mexiletine has been proposed as a gene-specific therapy for patients with LQTS type 3 caused by Na channelopathy. Mexiletine may shorten the QT interval and protect patients from arrhythmias at a mutation-specific fashion.^{13,14} However, we had found an unusual in utero presentation of intermittent AV block and ventricular tachycardia, spontaneously or lidocaine-induced, in a fetus and his sibling with LQTS.

We therefore investigated the mutations and the resultant electrophysiological properties of the channels.

METHODS

This study had been approved by the Institutional Committee on Human Research at this institution. The investigation conforms to the principles outlined in the Declaration of Helsinki.

Clinical Evaluation

Referred proband and eight family members underwent clinical evaluations and 12-lead electrocardiograms. The QT interval was measured on the lead II and corrected for the heart rate using Bazett's formula.

Mutational Analysis

Previously-published primer pairs were used to amplify all exons of KCNQ1, HERG, KCNE1, KCNE2, and SCN5A from genomic DNA. All of these exons were screened for the presence of nucleotide sequence polymorphisms by single-strand conformation polymorphism (SSCP). Amplification reactions were carried out using 40ng of template DNA, 8 pmol of primers, 2µl dNTPs (2.5 mM), 0.8µl Mg²⁺ (25 mM) and Taq polymerase. Then polymerase chain reaction (PCR) products were analysed by SSCP according to the manufacturer's protocol (GeneGel Excel®; Amersham Pharmacia Biotech, Uppsala, Sweden). When abnormal migration patterns were observed, PCR products were reamplified and sequenced by the dideoxynucleotide chain termination

method (DNA Sequencing Kit – BigDye Terminator Cycle Sequencing v 2.0, PE Biosystems) with fluorescent dideoxynucleotides on an ABI-Prism 373 DNA sequencer (Applied Biosystems), and the result was analysed with the Genotyper program (PE Biosystems).

Mutagenesis

For the hERG/F627L mutation, the site directed mutagenesis was performed on the hERG-pGH19 (6.9kb) construct provided by Dr. Gail A. Robertson (University of Wisconsin-Madison Medical School) with the following sense and anti-sense oligonucleotides, respectively (Underlined are mutated nucleotides):

5'-CTC ACC AGT GTG GGC CTC GGC AAC GTC TCT CCC-3' and

5'-GGG AGA GAC GTT GCC GAG GCC CAC ACT GGT GAG-3'

For Na_v1.5/R43Q, we used Na_v1.5 (hH1) and the following sense and anti-sense oligonucleotides, respectively (Underlined are mutated nucleotides):

5'-C ACC TTG CAG GAG AGC CAA GAG GGG CTG CCC GAG-3' and

5'-CTC GGG CAG CCC CTC TTG GCT CTC CTG CAA GGA C-3'

Mutagenesis was performed according to the Quick Change™ kit from Stratagene (La Jolla, CA). The mutated sites were confirmed by automatic sequencing. Capped mRNAs of wild type and mutated hERG were produced using the SP6 mMMESSAGE mMACHINE™ from Ambion (Austin, TX).

Preparation of *Xenopus* oocytes

Detailed preparation of *Xenopus* oocytes has been described previously.¹⁵ Briefly, oocytes were subjected to 2 mg/ml collagenase treatment for 2.5-3 hours, then stage V or VI oocytes were microinjected with 5 ng capped mRNA encoding either wild type (WT)

hERG, mutant hERG or both. The oocytes were maintained at 18°C in a 2-fold diluted solution of Leibovitz's L-15 medium (Gibco, Grand Island, N.Y., USA) enriched with 15 mM 4-(2-hydroxyethyl)-1-piperazine-methanesulfonic acid (HEPES, pH 7.6, adjusted with NaOH), 1 mM glutamine, and 50 µg/µl gentamycin. Oocytes were used for experimentation one to three days after injection.

The macroscopic K currents from the mRNA-microinjected oocytes were recorded using voltage-clamp technique with two 3M KCl-filled microelectrodes. Membrane potential was controlled by a Warner oocyte clamp (Warner Instrument Corp., Hamden, CT). Voltage commands were generated by computer using pCLAMP software version 5.5 (Axon Instruments, Inc., Foster City, CA). Currents were filtered at 2 kHz (-3 dB; 4 pole Bessel filter). Solutions used: The Ringer's bathing solution contained (mM): 116 NaCl, 2 KCl, 1.8 CaCl₂, 2.9 MgCl₂, 5 HEPES and pH was adjusted to 7.6 at 22°C with NaOH. All experiments were carried out at room temperature (22°C).

Transfection of tsA201 cell line

TsA201 is a mammalian cell line derived from human embryonic kidney HEK 293 cells by stable transfection with SV40 large T antigen.¹⁶ Macroscopic Na currents from tsA201-transfected cells were recorded using the whole-cell configuration of the patch clamp technique, as reported previously.^{17,18} Lidocaine was purchased from Sigma (St. Louis, MO, USA) and used at 10µM concentration.

Western blot analysis

The polyclonal anti-hERG antibody (rabbit hERGbasic) used in the present study was raised in rabbits against a C-terminal peptide corresponding to hERG aa residues 883-901 as described previously.¹⁹ Antiserum, hERGbasic, was purified on an affinity

column consisting of the C-terminal peptide used for immunization (aa 883-901: RQRKRKLSFRRRTDKDTEQ). Briefly, HEK/hERG cells were solubilized for 1h at 4°C in lysis buffer containing 150mM NaCl, 1mM EDTA, 50mM Tris, pH 8.0, 1% Triton X-100 and protease inhibitors (Complete, Roche Diagnostics, Indianapolis, IN). Protein concentrations were determined by the bicinchoninic acid (BCA) method (Pierce, Rockford, IL). Proteins were separated on sodium dodecyl sulfate (SDS) polyacrylamide gels, transferred to polyvinylidene difluoride membranes and developed using the hERGbasic antibody followed by ECL Plus (GE Healthcare, Piscataway, NJ).

Statistical Analysis

Data are expressed as mean \pm SEM (standard error of the mean). When indicated, a *t*-test was performed using statistical software in SigmaStat (Jandel Scientific Software, San Rafael, CA, USA). Differences were deemed significant at a *p* value < 0.05 .

RESULTS

Phenotypic Characterization

The clinical history has been described elsewhere.²⁰ In brief, the fetus was referred at the 25th gestational week due to intermittent AV block. Fetal echocardiography showed normal growth and cardiac structure. The atrial rate was 110-120/min and associated with a 3:2 AV block. The family history revealed that an uncle and an aunt had died of sudden death as well as a sibling with LQTS (Figure 1A). This sibling was noted to have had intermittent ventricular tachycardia and functional AV block during the fetal life, dying 3 days after birth. At the 26th gestational week, frequent 2:1 AV block and

non-sustained ventricular tachycardia was noted. At that time, we adopted a treatment strategy for perinatal onset LQTS, starting from lidocaine infusion to assess the potential benefit from mexiletine. Therefore, the mother under fetal echocardiographic monitoring received lidocaine intravenous infusion (10 µg/Kg/min). The fetus developed sustained ventricular tachycardia about 30 minutes after lidocaine infusion (Figure 2A). The tachycardia was converted to a 2:1 AV block only after discontinuing lidocaine (Figure 2B). At the 27th gestational week, incessant ventricular tachycardia (210-230/min) was noted. Subsequent maternal administration of propranolol controlled the tachycardia. The proband grew steadily and was delivered nearly at full term. The electrocardiogram after birth revealed sinus bradycardia (108/min) with a corrected QT interval of 0.60 sec (Figure 2C) and an intermittent 3:2 to 2:1 functional-AV block (Figure 2D). The functional AV block was related to an extremely prolonged QT interval that was not properly shortened with increasing heart rate. He subsequently received oral propranolol and nicorandil, and experienced no ventricular tachycardia. Evaluation at the age of five years revealed a well-developed child.

Genetic Characterization

SSCP analyses of KCNQ1, KCNE1 and KCNE2 revealed no abnormal conformers. Abnormal migration pattern was found in one fragment encompassing exon 7 of the HERG gene and one fragment encompassing exon 2 of the SCN5A gene. Sequence analyses of the hERG gene revealed a heterozygous mutation leading to a single base substitution (C¹⁸⁷⁹ →T), resulting in a Phe→Leu (F627L) substitution in the pore of the hERG channel. The F627L mutation was also found in the proband's father (Figure 1B). Sequence analyses of SCN5A gene showed another heterozygous mutation, G¹²⁸ →A,

resulting in a Gln→Arg (R43Q) substitution in the N-terminus (Figure 1B). Only the father had this second mutation. Both mutations were not identified in 100 unrelated, unaffected control individuals.

We also found three silent DNA changes that would not alter the amino acid sequence; one was located at SCN5A and two were at hERG: (1) C to T at position 5457 of SCN5A (distribution of genotypes in control group: CC: CT: TT= 0.18: 0.44: 0.38), (2) C to T at nucleotide position 1467 of hERG (distribution of genotypes in control group: CC: CT: TT= 0.14: 0.36: 0.50) and (3) C to T at position 1539 of hERG (distribution of genotypes in control group: CC: CT: TT= 0.21: 0.41: 0.38). These changes were benign single nucleotide polymorphisms, as they were seen in both the LQTS patient and the normal control population.

Biochemical and Biophysical Characterization of the Mutants

A western blot comparing hERG WT and hERG/F627L transiently expressed in HEK293 cells using Fugene revealed that the hERG/F627L expressed considerably less hERG protein, either in the fully glycosylated (fg) or core glycosylated (cg) form compared to the WT hERG protein (Figure 3). The blot showed also that fg was less pronounced demonstrating that there was also some trafficking deficiency of mutant HERG protein. These experiments were carried out in triplicates; therefore, the figure was representative of the data.

Capped mRNA encoding wild-type (hERG/WT) or mutant (hERG/F627L) potassium channels were injected separately or co-injected into *Xenopus laevis* oocytes. The resulting currents are illustrated in Figure 4. The injection of hERG/WT mRNA was followed two days later by a strong expression of the hERG/WT channel (Figure 4A).

However, oocytes injected with mRNA encoding the hERG/ F627L mutant channels exhibited K^+ currents of lower amplitude (Figure 4C) with altered I/V relation in response to the conditioning pulse and almost no current in the second pulse (Figure 4E and F). The co-injection of the same amount of both mRNAs resulted in a 50% decrease in K^+ current amplitude (Figure 4B). Furthermore, the currents exhibited similar voltage-dependence upon activation (Figures 4E and 4F).

$Na_v1.5/WT$ and $Na_v1.5/R43Q$ mutant channels were transfected with the auxiliary β_1 -subunit in tsA201 cells. The biophysical properties of $Na_v1.5/WT$ and $Na_v1.5/R43Q$ with and without lidocaine are summarized in Table 1. The resulting Na currents showed similar fast activation and inactivation kinetics. However, the mutant exhibited a unique left shift toward more hyperpolarized voltages of the activation curve and a pronounced block after lidocaine. There were no persistent late Na currents in either $Na_v1.5/WT$ or $Na_v1.5/R43Q$ (Figure 5). Illustrative whole-cell currents obtained in response to depolarizing steps between -100 and +50 mV are shown (Figure 6A). The I/V relationship was not significantly affected by this mutation, but lidocaine resulted in a left-shift of the I/V relations (Figure 6B).

Steady-state activation and inactivation were not significantly different between the wild type and the mutant (Figure 7A). Lidocaine at 10 μM concentration caused a left-shift of the inactivation in both, but the degree of shift was less in the mutant. In addition, an unusual left shift to hyperpolarizing voltages of the activation was only observed in the mutant (Figure 7A). Thereby, the window currents would be more in the mutant. Lidocaine slowed down the recovery of Na channels from inactivation, and the extent of suppression was greater in the mutant than in the wild-type form (Figure

7B and Table 1). Similarly, the use-dependent block by lidocaine was more pronounced in the mutant than in the wild-type form (Figure 8A, B and C).

DISCUSSION

In this study, we have identified novel compound hERG mutation and SCN5A variant in a family with LQTS. The SCN5A/R43Q variant was at the N-terminus region and is to date the only SCN5A variant that can result in latent lidocaine-induced phenotype of arrhythmia. Whereas the hERG/F627L mutation results in the phenotype of LQTS by decreased I_{Kr} , the SCN5A/R43Q variant, though it *per se* does not prolong repolarization, causes unusual hyperpolarizing shift of the activation kinetics and may attribute to the development of ventricular tachyarrhythmias after lidocaine.

Previously recognized SCN5A mutations causing LQTS mostly result in a persistent inward sodium current that can be ameliorated by sodium-channel blockers, including lidocaine.²¹ Clinical observations also advocate that lidocaine can effectively rescue patients of LQT3 from ventricular tachycardia.^{4,22} None of these SCN5A mutations have been associated with lidocaine-induced arrhythmia. Based on these observations, we had set a treatment strategy, starting with lidocaine infusion to assess the potential benefits from lidocaine and mexiletine, which had been also applied in this fetus through maternal administration. However, an unusual lidocaine-induced ventricular tachycardia was observed. We did not repeat the lidocaine infusion test again in the proband after birth because of medical ethic consideration. Nonetheless, the SCN5A R43Q variant, identified from this family, exhibits an unusual kinetics of the Na channels after lidocaine and is the first genetic variant responsible for latent lidocaine-induced phenotype of ventricular arrhythmia. The SCN5A R43Q variant *per se* behaves like the wild type. But, after lidocaine, the I/V curve shifts to the left, thereby increasing the availability of Na current at resting voltages and eliciting Na

current at a membrane potential around -60 mV. In fetuses, the membrane potential is less negative than in the adult and can approach this vulnerable voltage range.²³ In addition, the window current after lidocaine is also enhanced due to a hyperpolarizing (left) shift of the activation curve along with a lesser degree of left-ward shift of steady-state inactivation in the mutant. Although the lidocaine-induced use-dependent block was greater in the mutants, the difference was small at the heart rate of 230 bpm (3.9 Hz) which was the rate of clinical ventricular tachycardia in our patient. Thus, we may deduce that most of the lidocaine-induced increase in window current should remain under tachycardia, despite this use-dependent block. The increased availability of the Na current at the resting voltages after lidocaine in this variant will lower the threshold for regenerative depolarization of the membrane. As a consequence, a lower minimal fraction of recovery from inactivation shall be required for membrane excitability to be restored, which may shorten the refractory period. Owing to the hERG mutation-induced decrease in I_{Kr} current, a prolonged action potential plateau is maintained, with the known propensity to develop an extrasystole from early after-depolarizations. In this patient, with increased window currents and a shorter refractory period from SCN5A R43Q variant after lidocaine, such an extrasystole from early after-depolarizations due to prolonged action potential plateau from hERG/F627L mutant may lead to sustained ventricular reentry. Previously recognized mutations in the N-terminus region of SCN5A were identified in several patients with Brugada syndrome (R27H, G35S and R104Q) and in one elderly patient with LQTS (G9V).²⁶⁻²⁸ However, the structure-function studies of these mutations have not been carried out.

Compound mutations account for 4-8 % of the mutations identified in patients

with LQTS, but the functional studies had only rarely performed.¹⁰⁻¹² The compound mutations may involve the same or different LQTS genes (e.g., two independent KCNQ1 mutations, KCNQ1 + KCNH mutations, KCNQ1 + SCN5A mutations, or rarely hERG + SCN5A mutations).⁹⁻¹² Functional hERG channels develop from the co-assembly of four subunits into a tetrametric protein on the cell membrane. Each subunit contains six membrane-spanning domains (S1 to S6) flanked by Amino (N)- and Carboxyl (C)-terminus regions with the pore region extending from S5 to S6. Mutations over the pore regions account for about one third of the hERG mutations, commonly resulting in defective I_{Kr} channels and thereby a loss of function in I_{Kr} .^{29,30} The phenotypes of pore region mutations were associated with longer QT intervals and a higher risk of cardiac events as compared to non-pore region.²⁹ Compound mutations involving the hERG genes have been identified in pore and non-pore regions, with most of them associated with mutations on the KCNQ1 gene.^{10,12} Our patient is probably the first reported case with a hERG pore region mutation and a SCN5A variant with complex electrophysiological interaction other than additive prolongation of the repolarization.

In conclusion, we have identified a novel hERG/F627L mutation that results in LQTS with fetal onset of AV block and ventricular tachycardia. Besides, a coexisting SCN5A/R43Q variant, although it *per se* does not prolong repolarization, attributes the development of ventricular tachyarrhythmias after lidocaine. Patients with such latent lidocaine-induced phenotype given lidocaine or mexiletine may be at risk.

Acknowledgements

This study was supported in part by a grant from the Cardiac Children Foundation ROC (CCF0602). This study was also supported by grants from the Heart and Stroke Foundation of Québec (HSFQ), the Canadian Institutes of Health Research, MT-13181.

Dr M. Chahine is a J.C. Edwards Foundation Senior Investigator.

REFERENCES

1. Roberts R: Genomics and cardiac arrhythmias, *J Am Coll Cardiol* 2006;47:9-21.
2. Schwartz PJ: The congenital long QT syndromes from genotype to phenotype: clinical implications. *J Intern Med* 2006;259:39-47.
3. Lupoglazoff JM, Denjoy I, Villain E, et al.: Long QT syndrome in neonates: conduction disorders associated with HERG mutations and sinus bradycardia with KCNQ1 mutations. *J Am Coll Cardiol* 2004;43:826-30.
4. Chang CC, Acharfi S, Wu MH, et al.: A novel SCN5A mutation manifests as a malignant form of long QT syndrome with perinatal onset of tachycardia/bradycardia. *Cardiovasc Res* 2004;64:268-78.
5. Lehnart SE, Ackerman MJ, Benson Jr DW, et al.: Inherited arrhythmias. A National Heart, Lung, and Blood Institute and Office of Rare Diseases workshop consensus report about the diagnosis, phenotyping, molecular mechanisms, and therapeutic approaches for primary cardiomyopathies of gene mutations affecting ion channel function. *Circulation* 2007;116:2325-45.
6. Wang Q, Shen J, Splawski I, et al: SCN5A mutations associated with an inherited cardiac arrhythmia, long QT syndrome. *Cell* 1995;80:1-20.
7. Curran ME, Splawski I, Timothy KW, et al: A molecular basis for cardiac arrhythmia: HERG mutations cause long QT syndrome. *Cell* 1995;80:795-803.
8. Schulze-Bahr E, Fenge H, Eitzrodt D, et al.: Long QT syndrome and life threatening arrhythmia in a newborn: molecular diagnosis and treatment response. *Heart* 2004;90:13-16.
9. Westenskow P, Splawski I, Timothy KW, et al.: Compound mutations: a common

- cause of severe long-QT syndrome. *Circulation*. 2004;109:1834–41.
10. Wang Z, Li H, Moss AJ, et al: Compound heterozygous mutations in KVLQT1 cause Jervell and Lange-Nielson syndrome, *Mol Gen Meta* 2002;75:308-316.
 11. Lasen LA, Fosdal I, Anderson PS, et al.: Recessive Romano-Ward syndrome associated with compound heterozygosity for two mutations in the KVLQT1 gene. *Eur J Hum Genet*. 1999;7:724–8.
 12. Yamaguchi M, Shimizu M, Ino H, et al.: Compound heterozygosity for mutations Asp(611)Tyr in KCNQ1 and Asp(609)Gly in KCNH2 associated with severe long QT syndrome. *Clin Sci (Lond)*. 2005;108;143–50.
 13. Shimizu W, Aiba T, Antzelevitch C. Specific therapy based on the genotype and cellular mechanism in inherited cardiac arrhythmias. Long QT syndrome and Brugada syndrome. *Curr Pharm Des* 2005;11:1561-72.
 14. Ruan Y, Liu N, Bloise R, et al.: Gating properties of SCN5A mutations and the response to mexiletine in long-QT syndrome type 3 patients. *Circulation* 2007; 116;1137-44.
 15. Chahine M, Chen LQ, Barchi RL, et al.: Lidocaine block of human heart sodium channels expressed in *Xenopus* oocytes. *J Mol Cell Cardiol*. 1992;24:1231-6.
 16. Margolskee RF, McHendry-Rinde B, Horn R: Panning transfected cells for electrophysiological studies. *Biotechniques* 1993;15:906-11.
 17. Keller DI, Acharfi S, Delacretaz E, et al.: A novel mutation in SCN5A, delQKP 1507-1509, causing long QT syndrome: role of Q1507 residue in sodium channel inactivation. *J Mol Cell Cardiol* 2003;35:1513-21.
 18. Hamill OP, Marty A, Neher E, et al.: Improved patch-clamp techniques for

high-resolution current recording from cells and cell-free membrane patches,
Pflügers Arch 1981;391:85-100.

19. Roti EC, Myers CD, Ayers RA, et al.: Interaction with GM130 during HERG ion channel trafficking. Disruption by type 2 congenital long QT syndrome mutations. Human Ether-à-go-go-Related Gene. J Biol Chem 2002;277:47779-85.
20. Chang IK, Shyu MK, Lee CN, et al.: Prenatal diagnosis and treatment of fetal long QT syndrome: a case report. Prenatal Diag 2002;22:1209-12.
21. Tan HL: Sodium channel variants in heart disease: expanding horizons. J Cardiovasc Electrophysiol 2006;17: S151-157.
22. Betrian Blasco P, Antunez Jimenez MI, Falcon Gonzalez LH, et al.: Neonatal life-threatening arrhythmia responding to lidocaine, a probable LQTS3. Int J Cardiol 2007;117:e61-3.
23. Wu MH, Su MJ, Lue HC: Age-related quinidine effects on ionic currents of rabbit cardiac myocytes. J Mol Cell Cardiol. 1994;26:1167-77.
24. Levy-Nissenbaum E, Eldar M, Wang Q, et al.: Genetic analysis of Brugada syndrome in Israel: two novel mutations and possible genetic heterogeneity. Genet Test 2001;5:331-4.
25. Millat G, Chevalier P, Restier-Miron L, et al.: Spectrum of pathogenic mutations and associated polymorphisms in a cohort of 44 unrelated patients with long QT syndrome. Clinical Genetics 2006;70: 214-27.
26. Priori SG, Napolitano C, Gasparini M, et al.: Natural history of Brugada syndrome: insights for risk stratification and management. Circulation. 2002;105:1342-47.
27. Vatta M, Dumaine R, Antzelevitch C, et al.: Novel mutations in domain I of

- SCN5A cause Brugada syndrome. *Mol Genet Metab* 2002;75:317–24.
28. Splawski I, Shen J, Timothy KW, et al.: Spectrum of mutations in long-QT syndrome genes. KVLQT1, HERG, SCN5A, KCNE1, and KCNE2, *Circulation*. 2000;102:1178-85.
 29. Moss AJ, Zareba W, Kaufman ES, et al.: Increased risk of arrhythmic events in long-QT syndrome with mutations in pore region of the human ether-a-go-go-related gene potassium channel. *Circulation*. 2002;105:794-9.
 30. Sanguinetti MC, Curran ME, Spector PS, et al.: Spectrum of HERG K⁺-channel dysfunction in an inherited cardiac arrhythmia. *Proc Natl Acad Sci USA*. 1996;93:2208-12.

Figure legends

Figure 1. (A) Pedigree of the study family is depicted. The open circles/squares indicate unaffected women and men, respectively, and the closed circles/squares indicate affected women/ men, respectively. The arrow indicates the proband. Individuals are assigned as affected (black), unaffected (white), or uncertain phenotypes (gray). Genotypes are shown beside each symbol. (B) DNA sequence chromatograms showing the HERG heterozygous mutation with a C to T transition (arrow) resulting in a phenylalanine to leucine substitution at codon 627, and the SCN5A heterozygous mutation with a G to A transition (arrow) resulting in an arginine to glutamine substitution at codon 43 in the proband and his father. The results from his mother and brother were normal.

Figure 2. (A) The M-mode fetal echocardiogram is depicted positioned to simultaneously record the left ventricle (V) and left atrium (A). Ventricular tachycardia was impressed due to the rapid ventricular rate with dissociated ventriculo-atrial conduction. (B) After discontinuing lidocaine, the tachycardia stopped, and the rhythm showed an atrial rate of 130/min that conducted to the ventricle in a 2:1 fashion. (C) The standard electrocardiogram taken soon after birth. Paper speed 25 mm/sec; 1 mV = 10 mm. The corrected QT interval at a sinus rate of 104/min was 0.60 sec, and the T wave was broad. (D) On the same day, when the sinus rate accelerated to 140/min, a 2:1 pseudo-atrioventricular block developed due to an extremely prolonged QT interval.

Figure 3. Depiction of western blot comparing hERG WT and hERG/F627L transiently expressed in HEK293 cells using Fugene. HEK293 cells were transfected with different amounts of cDNA, 0.75 and 1 μ g. hERG WT is expressed as a fully glycosylated, mature 160-kDa form (fg) and a core-glycosylated, ER resident 135-kDa form (cg). As can be seen, hERG/F627L expresses considerably less hERG protein in the fully glycosylated (fg) or core glycosylated (cg) forms than in the WT hERG protein.

Figure 4. hERG potassium currents are depicted as recorded from *Xenopus* oocytes injected with cRNA encoding for either (A) hERG/WT or (C) hERG/F627L or co-injected with (B) hERG/WT and hERG/F627L or (D) non-injected. Potassium currents were elicited from a holding potential of -80mV with a 2-second test pulse duration, beginning at -80 mV to +60 mV in 10 mV increments followed by a step potential of 2 seconds to evoke tail currents. In (C), no current was recorded from oocytes injected with mRNA encoding hERG/F627L only. The I/V relation in response to the conditioning pulse (E) and in the second pulse (F) were summarized.

Figure 5. The persistent sodium currents from Nav1.5/WT and Nav1.5/R43Q are depicted. Currents were generated from a holding potential of -140 mV to -10 mV for 400 ms. Dashed line represents zero currents. After 5 μ M TTX treatment, both currents from Nav1.5/WT and Nav1.5/R43Q were blocked.

Figure 6. Analysis of whole-cell currents recorded from tsA201 cell line expressing $\text{Na}_v1.5/\text{WT}$ and $\text{Na}_v1.5/\text{R43Q}$ with and without lidocaine are depicted. **(A)** Families of whole-cell currents from $\text{Na}_v1.5/\text{WT}$, $\text{Na}_v1.5/\text{R43Q}$, $\text{Na}_v1.5/\text{WT}$ with lidocaine, and $\text{Na}_v1.5/\text{R43Q}$ with lidocaine are depicted. I_{Na} was elicited by depolarizing pulses from -100 mV to +50 mV in 10 mV increments. The holding potential was -140 mV. The protocol is shown in panel **(B)**. **(B)** Current-voltage relationships of $\text{Na}_v1.5/\text{WT}$ (\circ , $n=9$), $\text{Na}_v1.5/\text{R43Q}$ (\bullet , $n=9$), $\text{Na}_v1.5/\text{WT}$ with lidocaine (Δ , $n=7$), and $\text{Na}_v1.5/\text{R43Q}$ with lidocaine (\blacktriangle , $n=9$) are depicted. The current amplitude was normalized to the cellular membrane capacitance. The curve for $\text{Na}_v1.5/\text{R43Q}$ with lidocaine was significantly shifted to negative potentials. There was no significant difference for current densities among the currents of $\text{Na}_v1.5/\text{WT}$ and $\text{Na}_v1.5/\text{R43Q}$ with and without lidocaine.

Figure 7. The gating properties of steady state activation, inactivation, and recovery from inactivation are depicted. **(A)** Effects of $10\mu\text{M}$ lidocaine on steady-state activation are depicted: (Δ for $\text{Na}_v1.5/\text{WT}$, $n=7$; \blacktriangle for $\text{Na}_v1.5/\text{R43Q}$, $n=8$; \square for $\text{Na}_v1.5/\text{WT}$ with lidocaine, $n=9$; \blacksquare for $\text{Na}_v1.5/\text{R43Q}$ with lidocaine, $n=8$) and inactivation (\circ for $\text{Na}_v1.5/\text{WT}$, $n=8$; \bullet for $\text{Na}_v1.5/\text{R43Q}$, $n=7$; \diamond for $\text{Na}_v1.5/\text{WT}$ with lidocaine, $n=7$; \blacklozenge for $\text{Na}_v1.5/\text{R43Q}$ with lidocaine, $n=8$). Activated currents were generated from a holding potential of -140 mV, following 50 ms voltage steps from -100 to +20 mV in 10 mV increments (See protocol as inset.). There was an 11 mV shift for $\text{Na}_v1.5/\text{R43Q}$ to negative potentials after lidocaine. Voltage-dependence of inactivation was obtained by

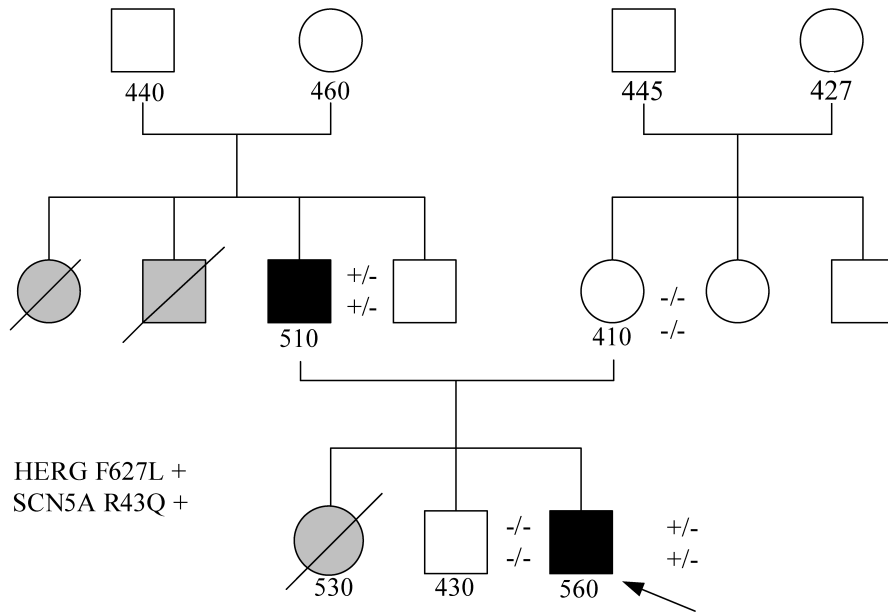
measuring the peak Na^+ current during a 20 ms test pulse of -30 mV, which followed a 500 ms pre-pulse to membrane potentials between -140 and -30 mV from a holding potential of -140 mV (See protocol as inset.). After **10 μM** lidocaine treatment, the curves of both $\text{Na}_v1.5/\text{WT}$ and $\text{Na}_v1.5/\text{R43Q}$ were shifted to negative potentials, but there was no significant difference between them. The data were fitted to a Boltzman equation with parameters shown in table 1. (B) Effects of **10 μM** lidocaine on recovery from inactivation (\circ for $\text{Na}_v1.5/\text{WT}$, n=7; \bullet for $\text{Na}_v1.5/\text{R43Q}$, n=7; Δ for $\text{Na}_v1.5/\text{WT}$ with lidocaine, n= 8; \blacktriangle for $\text{Na}_v1.5/\text{R43Q}$ with lidocaine, n= 9) are depicted. A 500 ms conditioning pre-pulse was used to monitor recovery by a 20 ms test pulse after a variable recovery interval from 1-2000 ms (see protocol as inset). The time constants (shown in table 1) were yielded by a two-exponential function, $y = A_1 \times (1 - \exp[-t/\tau_1]) + A_2 \times (1 - \exp[-t/\tau_2])$. The time constants for both $\text{Na}_v1.5/\text{WT}$ and $\text{Na}_v1.5/\text{R43Q}$ after lidocaine were slower than those of $\text{Na}_v1.5/\text{WT}$ and $\text{Na}_v1.5/\text{R43Q}$ before lidocaine, but there was no significant difference between them (Data are shown in Table 1).

Figure 8. Effects of frequency-dependent inhibition by lidocaine are depicted.

(A) Frequency-dependent inhibition of $\text{Na}_v1.5/\text{WT}$ and $\text{Na}_v1.5/\text{R43Q}$ sodium currents with and without **10 μM** lidocaine is depicted. A train of 50 pulses was applied at 40 mV and -30 mV at frequencies between 10 and 100 Hz. The peak currents elicited by each test pulse were normalized to the current of the first pulse P_n/P_1 (where n = 1-50) and were plotted versus the pulse number (See inset.). The pulse duration was 8 ms. The holding and interpulse potentials were -140 mV. (B) Ratio of the currents elicited by the 50th and first pulses (P_{50}/P_1) versus the pulsing frequency is depicted. The current of

Na_v1.5/WT was inhibited by lidocaine. There was a further reduction for Na_v1.5/R43Q after lidocaine. (C) Representative raw current traces of Na_v1.5/WT and Na_v1.5/R43Q stimulated at 50 Hz with and without 10μM lidocaine are depicted (***p* < 0.01 versus Na_v1.5/WT; ##*p* < 0.01 versus Na_v1.5/WT with lidocaine).

A



B

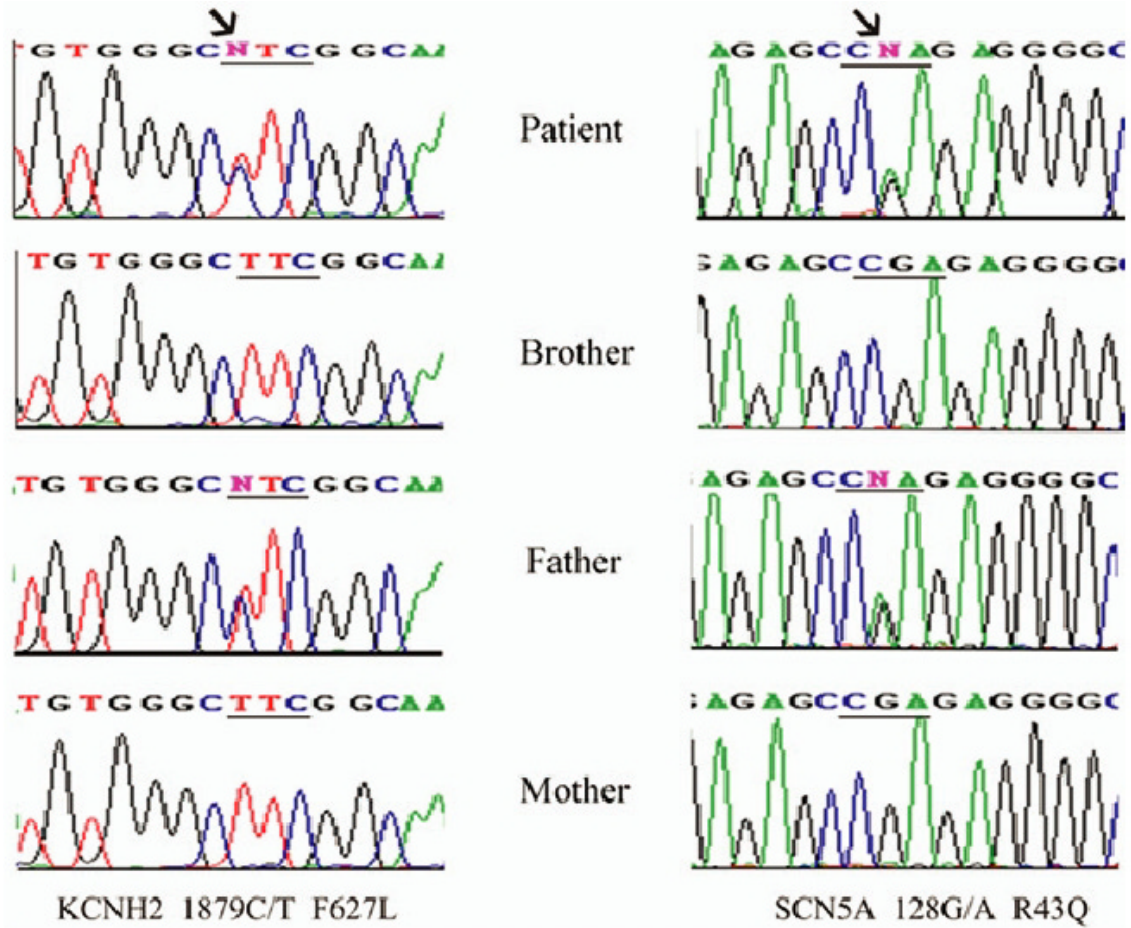


Figure 1

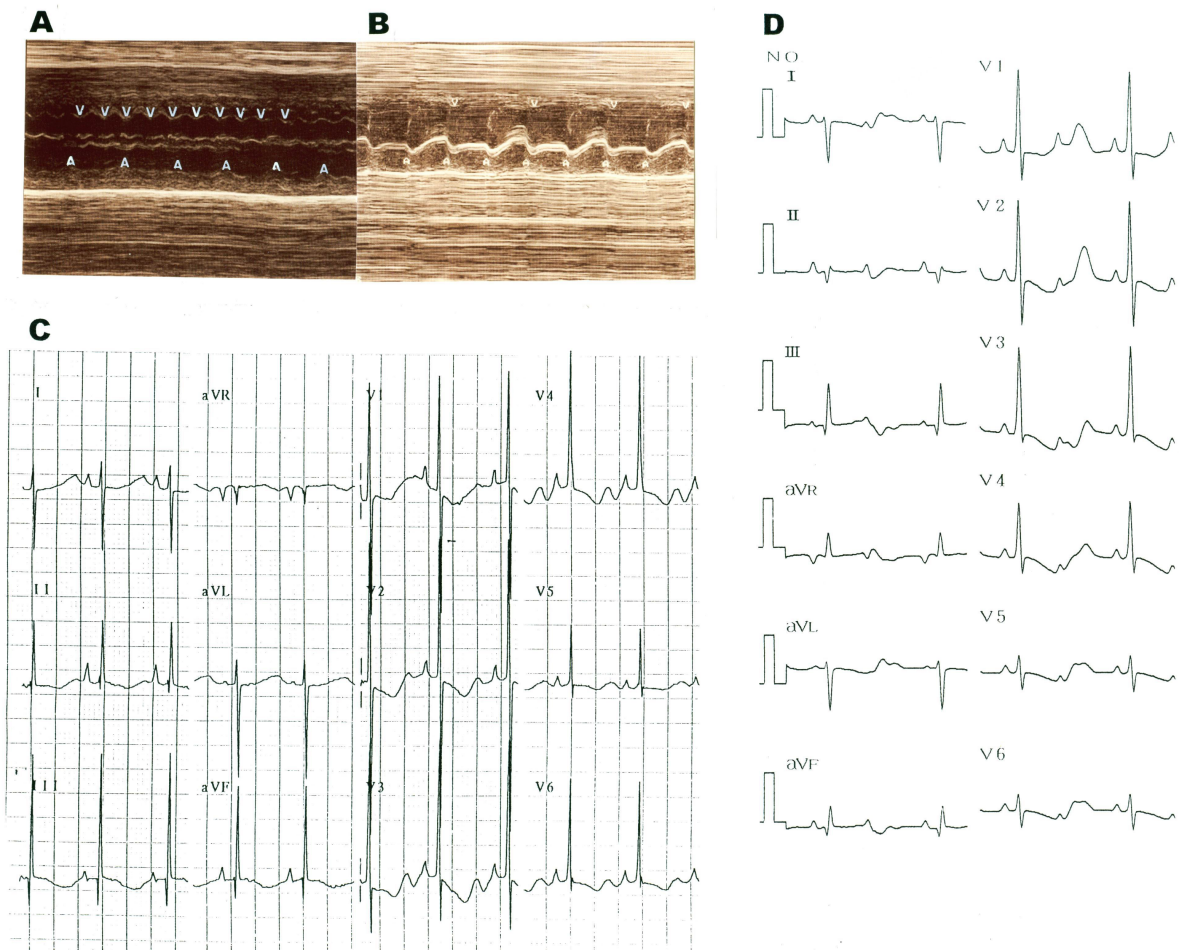


Figure 2

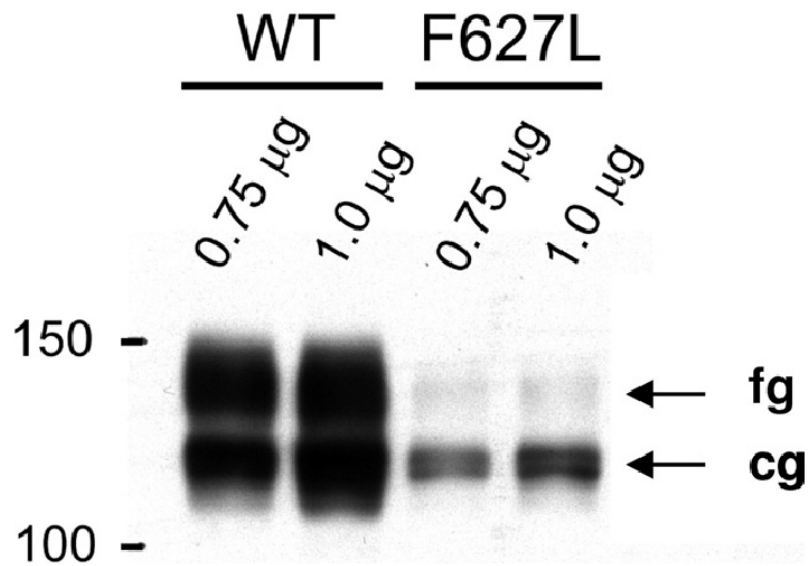


Figure 3

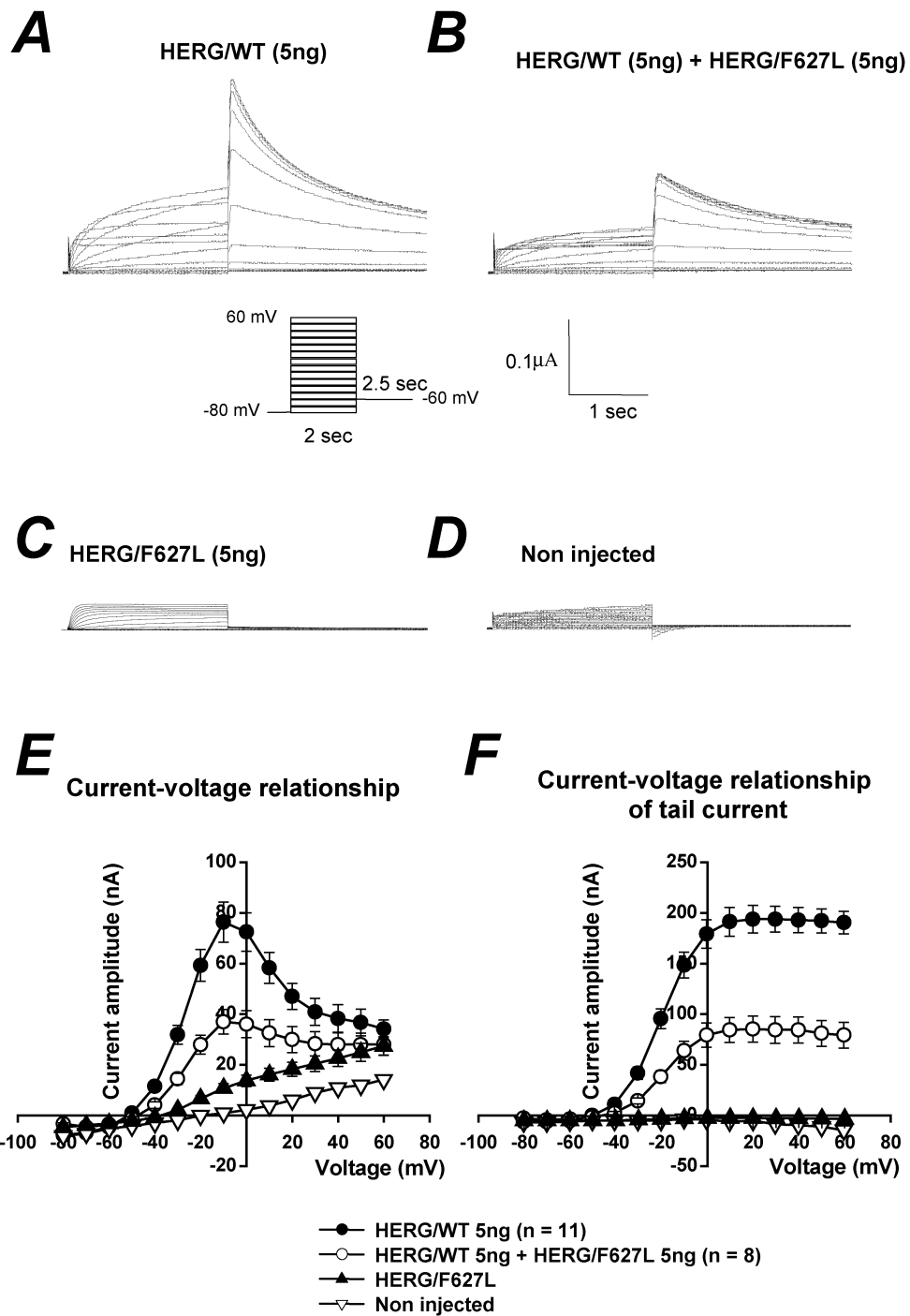


Figure 4

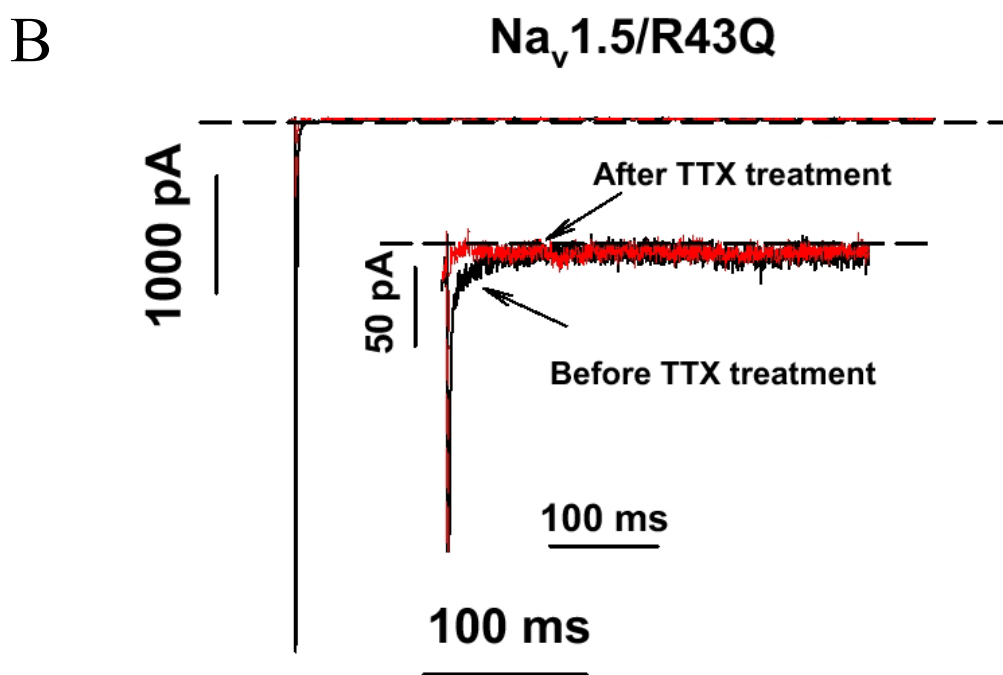
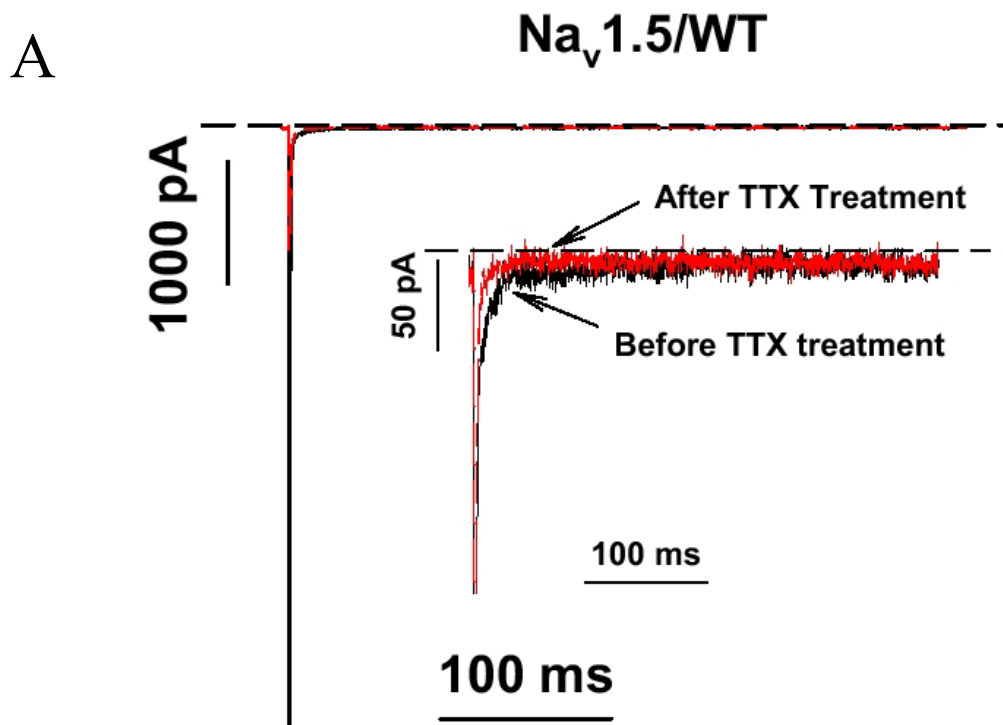
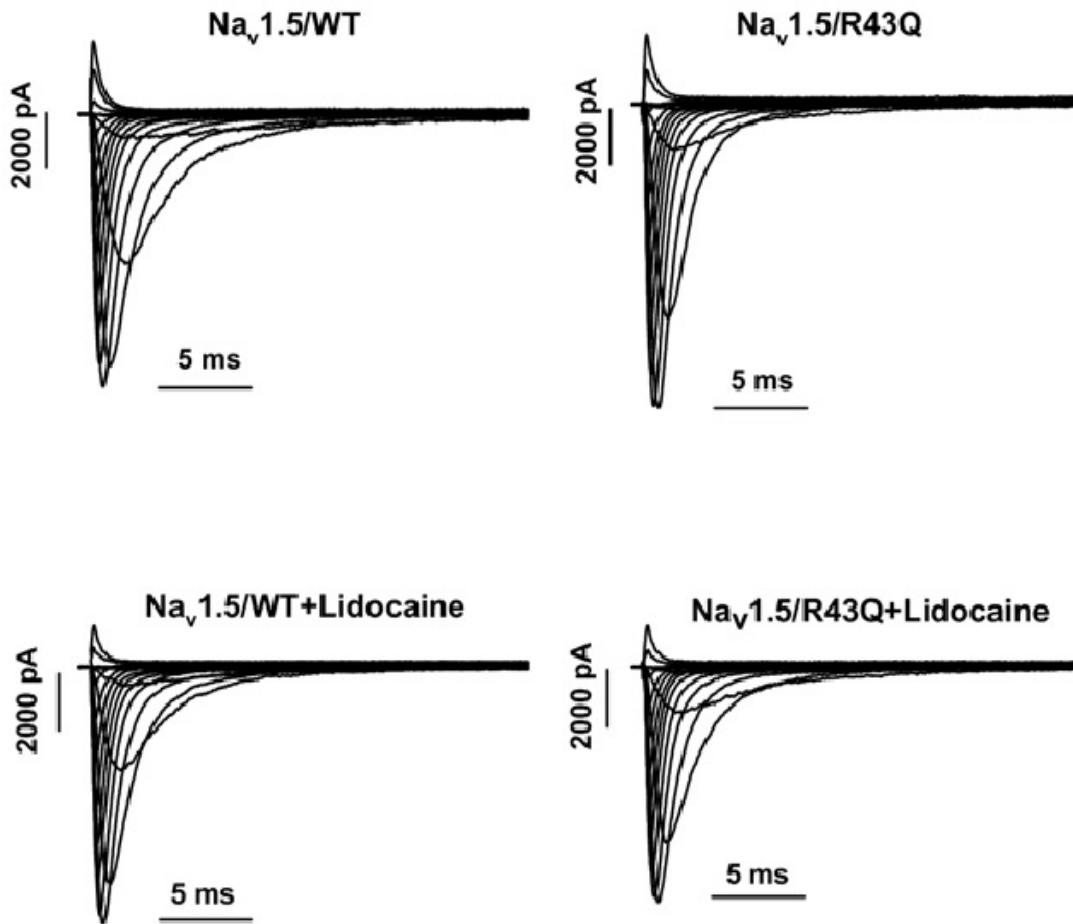


Figure 5

A



B

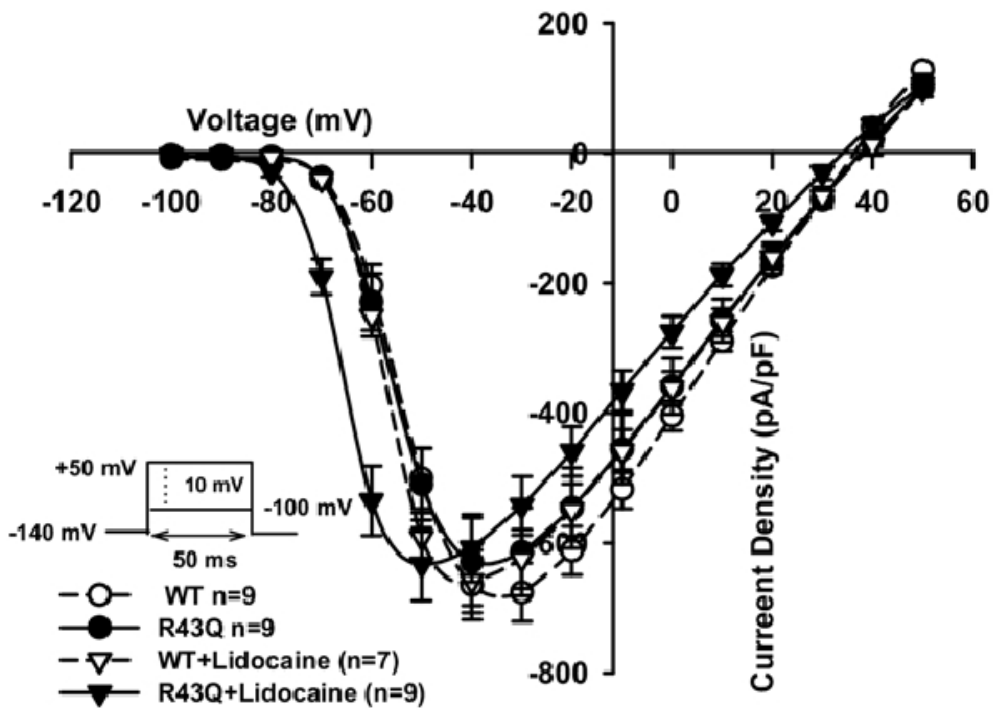
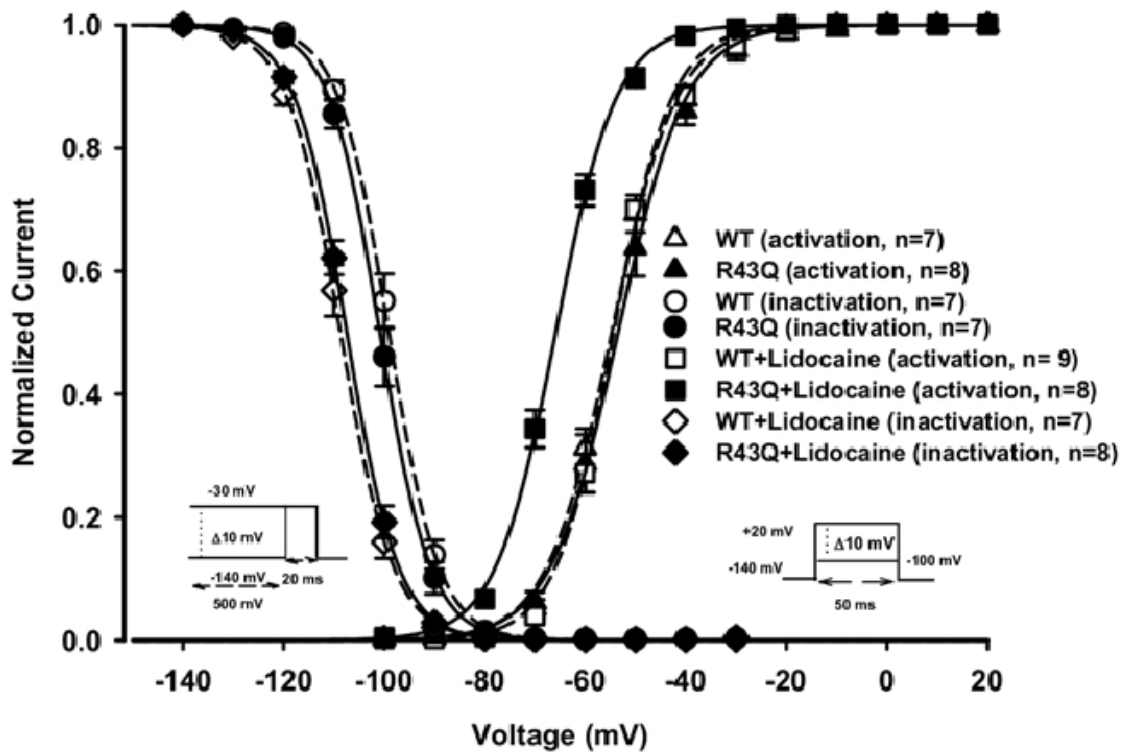


Figure 6

A



B

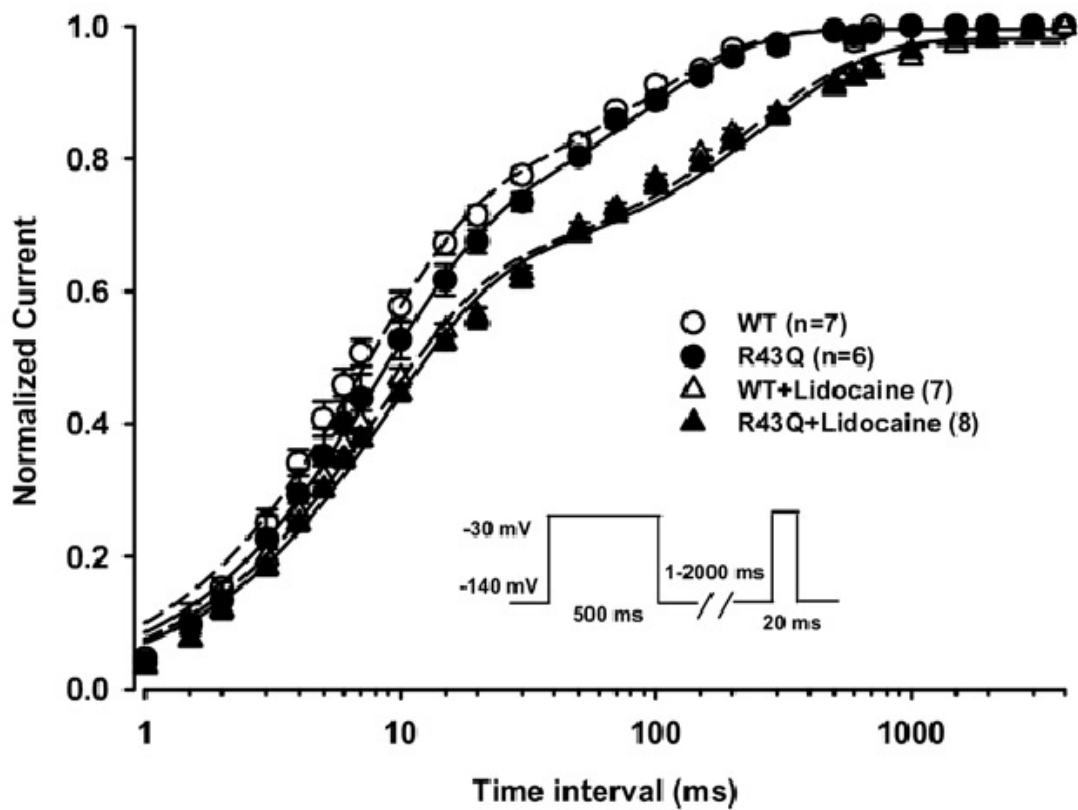


Figure 7

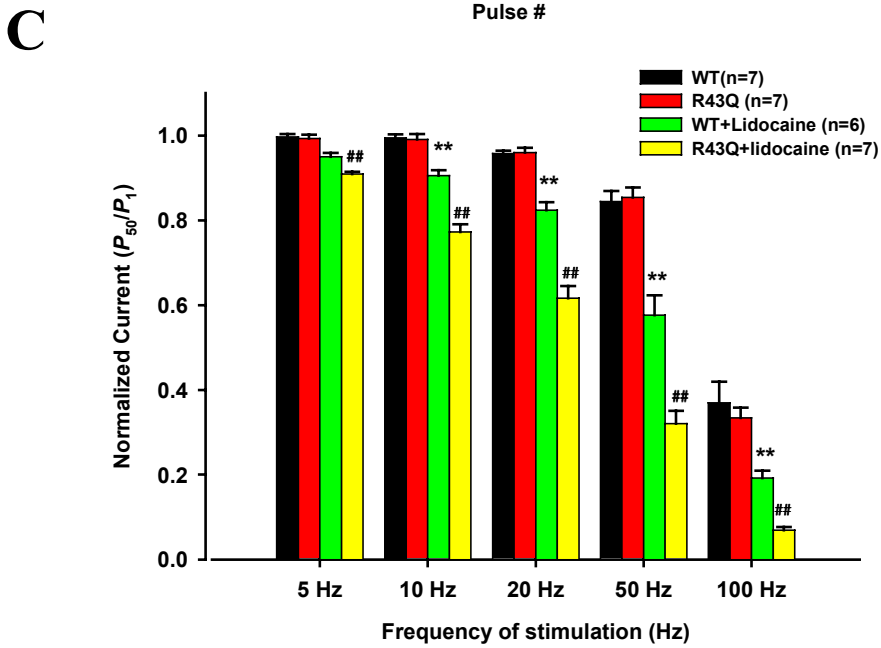
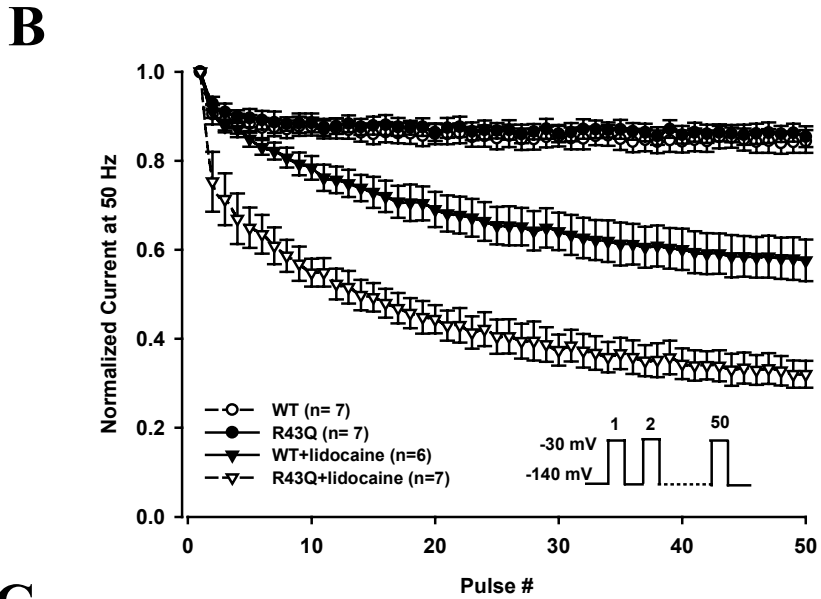
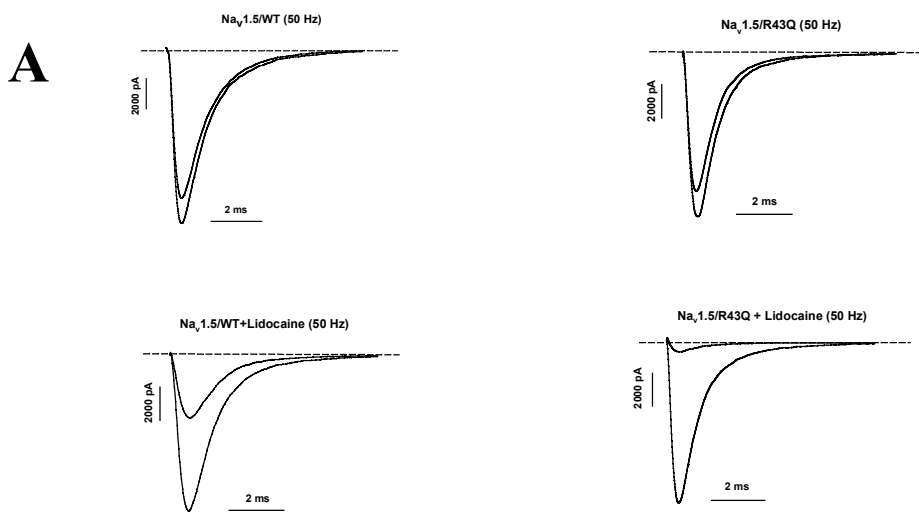


Figure 8